Mat. Res. Soc. Symp. Proc. Vol. 635 © 2001 Materials Research Society

# Fabrication and Characterization of Chromium Oxide Nanoparticles/Thin Films

**Zhenchen Zhong**
Institute for Micromanufacturing (IfM) and Physics Program, Louisiana Tech University, Ruston, LA 71272; U.S.A.
and Department of Physics, Grambling State University, Grambling, LA 71245, U.S.A.
**Ruihua Cheng**
Department of Physics and Astronomy and the Center for Materials Research and Analysis (CMRA), Behlen Laboratory of Physics, University of Nebraska-Lincoln, NE 68588-0111, U.S.A.

## ABSTRACT

Well-dispersed nanoscale textured chromium oxide particles/thin films can be fabricated under certain conditions by laser-induced solution deposition (LISD) from organic solutions and by using selective organometallic chemical vapor deposition (OMCVD). The fabricated nanoparticles/thin films are characterized by scanning electron microscope (SEM), EDX, X-ray diffraction, and magnetic measurements. We have successfully demonstrated that the LISD and OMCVD are unique techniques for fabricating uniformly-distributed thin films but anistropic chromium oxide particles, which can be used in electro-magnetic devices. The magnetization measurements show that both types of chromium oxides are presented and that the Curie temperature $T_c$ and the saturation magnetization field may be adjustable by controlling the stoichiometry.

## INTRODUCTION

Spin-tunnel junctions, spin-vlaves [1] and other magnetoresistive devices [2,3] have aroused wide interests because of their importance in science and technology. These so-called spin-dependent devices, i.e., spintronics depend upon spin-polarized electrons rather than bias voltages or currents. They are new generation microelectronics, in other words, nanoelectronics. Chromium oxides are promising candidates because of their half-metallic properties and high spin-polarization. The insulating antiferromagnetic chromium oxide $Cr_2O_3$ has a Neél temperature $T_N$ (i.e., the similar Curie temperature for the antiferromagnetic case) 307 K and is suitable for tunnel junction barrier [3] both below and above the Neél temperature. The ferromagnetic chromium oxide $CrO_2$ with $T_c$ 397 K [4] has been predicted to be half-metallic (metallic for one spin direction while insulating for the other spin direction) by band structure calculations [5-9], though Kulatov and Mazin found $CrO_2$ to be insulating in both spin-directions [10]. Evidence of 80 to 100% polarization, consistent with the half metallic character of $CrO_2$, were observed in many experimental measurements such as spin-polarized photoemission [11], vacuum tunneling [12], and Andreev scattering [13,14]. The high electron polarization, in addition to the half metallic character of the surface [9] makes $CrO_2$ an attractive material for spin-polarized electron tunneling. Very large spin-dependent tunneling (junction) magnetoresistance (TMR) made of $CrO_2$ is expected.

Therefore $CrO_2$ is a material of interest for spin-polarized electronics (i.e., spintronics) because of the spin-polarization in this material approaching unity. Another reason for using $CrO_2$ in spintronics is that it is possible to make all magnetic oxide spin-dependent tunnel

junctions. In this case the tunnel barrier is likely to be a native $Cr_2O_3$ layer sandwiched in-between the two $CrO_2$ layers. The research for making $CrO_2/Cr_2O_3/CrO_2$ tunnel junctions is in progress, which will be reported elsewhere.

It is difficult to fabricate $CrO_2$ ultrathin films/nanoparticles using conventional methods because $CrO_2$ is metastable. However, it is good thing in some cases because the two phases $CrO_2/Cr_2O_3$ system exhibits higher magnetoresistance than the pure material [3]. The oxidation of the organometallic complex hexacarbonyl $Cr(CO)_6$ has the potential for selective deposition of $CrO_2$ [15-17]. These studies have established that chromium oxides are the thermodynamic sinks of chromium hexacarbonyl decomposition [17] and the oxidation is further aided by the presence of an ambient oxygen background [15,16]. By modifying this organometallic chemical vapor deposition (OMCVD) procedure, we have been able to fabricate the ferromagnetic and antiferromagnetic chromium oxides. Meanwhile we have used a counterpart laser-induced deposition in solution (LISD) to fabricate magnetic nanoparticle oxides. However, the precursor $Cr(CO)_6$ did not work in solution deposition as we expected. By error and try, we found that $CrCl_2$ was a choice as the solute of the deposition solution. In this paper we describe both the formation and the magnetic properties of these ultrathin films/nanoparticles by both vapor and solution deposition induced by laser.

## EXPERIMENTAL DETAILS

The growth of the chromium oxide films/nanoparticles by OMCVD were carried out on Si(111) substrates in an ultra high vacuum chamber, maintained at a base pressure at $1.0^{-9}$ torr or less. This chamber was designed for laser initiated chemical vapor deposition as described elsewhere [18,19]. The photolytic decomposition and oxidation of $Cr(CO)_6$ was performed by a commercial nitrogen laser with the main emission line at 337 nm (corresponding to 3.69 eV). The ambient oxygen ($O_2$) atmosphere was varied from $1x10^{-7}$ to $1x10^{-5}$ torr relative to the $Cr(CO)_6$ partial pressure of $1x10^{-5}$ torr, uncorrected for ionization gauge cross-section and monitored with a quadruple mass spectrometer operated in pulse counting mode.

The deposition of chromium oxides by laser-induced solution deposition (LISD) (the experimental system of LISD is described elsewhere [20]) were carried out by an argon ion-laser (the Coherent Innova 90 Series Ion Laser). The deposition solution was $CrCl_2$ dissolved in solvents containing various mixtures of methanol, cyclohexane, tetrohydrofuran (THF), and diethlether. The deposition time in this experiment varies from 0.5 hour to 24 hours. Both visible (laser power: 5-7 W and wavelength : 514 nm (457 – 528 nm) and UV radiation (laser power: 5-7 W and wavelength : 351 nm) were used in the experiment. The substrates for deposition were Si (111) wafers and sodium-glasses in all the experiments.

## RESULTS AND DISCUSSION

The SEM microscope of the thin film/nanoparticles, fabricated with $1x10^{-6}$ torr $O_2$ partial pressure and $1x10^{-5}$ torr $Cr(CO)_6$ partial pressure, is shown in Figure 1. The topology of the film is relatively uniform, with only a fine microstructure visible on the scale of 800 nm.

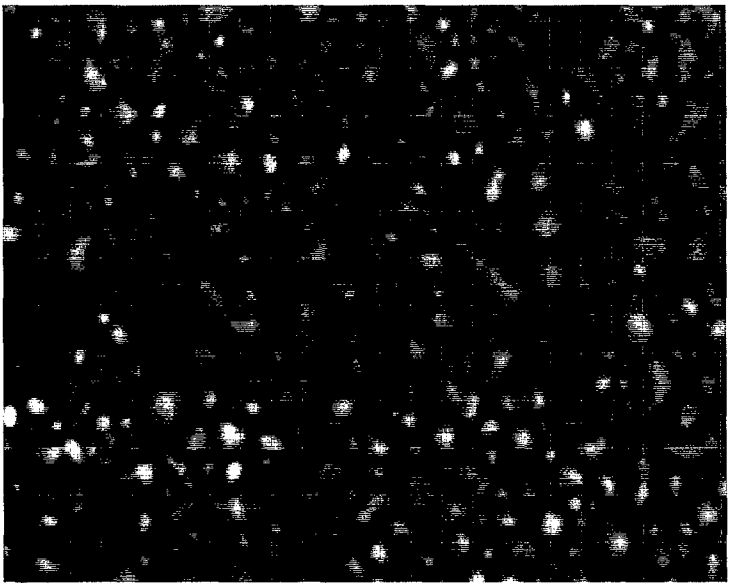

**Figure 1.** The scanning electron microscope image of a chromium oxide thin film/nanoparticles fabricated on Si (111) substrate through laser-initiated decomposition of $Cr(CO)_6$ (pressure $1x10^{-5}$ torr) in an ambient atmosphere of $O_2$ ($1x10^{-6}$ torr) as background.

The EDX spectra of the same thin film/nanoparticles in different areas provide evidence for the desirable oxygen and chromium signal in addition to the strong Si signal coming from the Si (111) substrate. We have done many spectra for the deposited thin films/nanoparticles. The results are quite similar, showing both peaks of chromium and oxygen.

Figure 2 shows the magnetization versus temperature obtained from superconducting quantum interference devices (SQUID) magnetometer. The inserted figures are Auger electron spectroscopy (AES). The critical temperature clearly depends upon the experimental conditions, especially the oxygen partial pressure at the time of thin film/nanoparticle fabrication. At $2x10^{-7}$ torr oxygen partial pressure relative to the $Cr(CO)_6$ partial pressure of $1x10^{-5}$ torr the Curie temperature was $345\pm10$ K. At the higher $1x10^{-6}$ torr oxygen partial pressure (relative to the $Cr(CO)_6$ partial pressure of $1x10^{-5}$ torr) the Curie temperature was about $390\pm10$ K. The absence of a sharp $T_c$ and the presence of a long tail in the magnetization curves (Figure 2), near the critical temperature, indicate positively a two phases system. The amount of $CrO_2$ phase increases with the $O_2$ partial pressure and the critical temperature approaches finally the expected $T_c$ of $CrO_2$ [4]. The samples characterized by Auger electron spectroscopy (AES), as shown in the insets of Figure 2, (A) presents the Auger spectrum characteristic to a $Cr_2O_3$ rich sample, and

(B) for a $CrO_2$ rich sample. The spectra show clearly that the Cr signal increases relative to the overlapping oxygen signal for the $Cr_2O_3$ samples as compared to the $CrO_2$ samples.

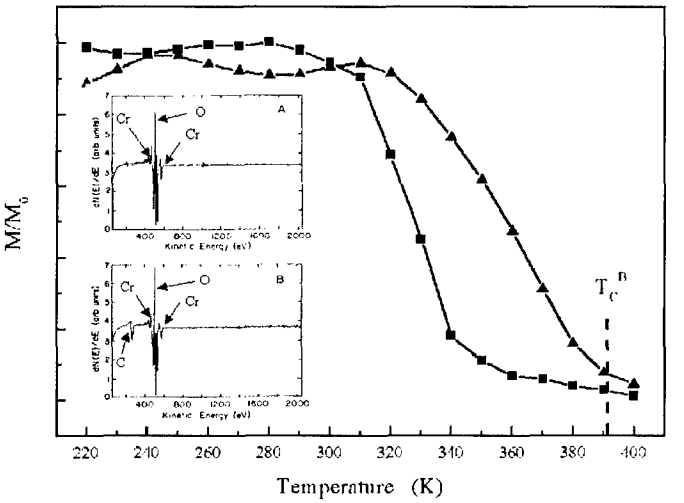


**Figures 2.** The magnetization (M) versus temperature (T) at an applied field of H=500 Oe. Data are shown for two thin films/nanoparticles: the data (∇) were taken from the film fabricated in an $O_2$ pressure of $2x10^{-7}$ torr relative to the $Cr(CO)_6$ partial pressure of $1x10^{-5}$ torr, while the data ( ) were taken from the film fabricated in an $O_2$ pressure of $1x10^{-6}$ torr relative to the $Cr(CO)_6$ partial pressure of $1x10^{-5}$ torr. Auger electron spectra of the photolytic oxidative chemical vapor deposition of $Cr_2O_3$ and $CrO_2$ (for high and low $O_2$ partial pressure respectively) are shown as insets A and B respectively.

As contrast, the growth of chromium oxides in the laser-induced solution deposition is usually islands growth mode rather than that of layer-by-layer growth (usually into films) in vapor deposition. The precursor $Cr(CO)_6$ worked fine in vapor deposition did not appear to be effective in solution deposition. Figure 3 shows the scanning electron microscope of the textured $CrO_x$ nanoparticles obtained by laser-induced deposition in solution (LISD) and the distribution of nanoparticles in the center of 230 nm in diameter. The experimental conditions for this sample are laser wavelength was at 514 nm in visible regime; laser beam exposure area was about 10 mm; solute was $CrCl_2$ (2.0 mg) dissolved in solvents of 1.5 ml THF and 1.5 ml cyclohexane; and the deposition time was twelve hours. The dominant particle size ($CrO_x$) was about 230 nm in diameter and there are also those bi-grains and triple-grains with 350 nm and 400 nm in diameter. The distribution shows uniform and appears textured.

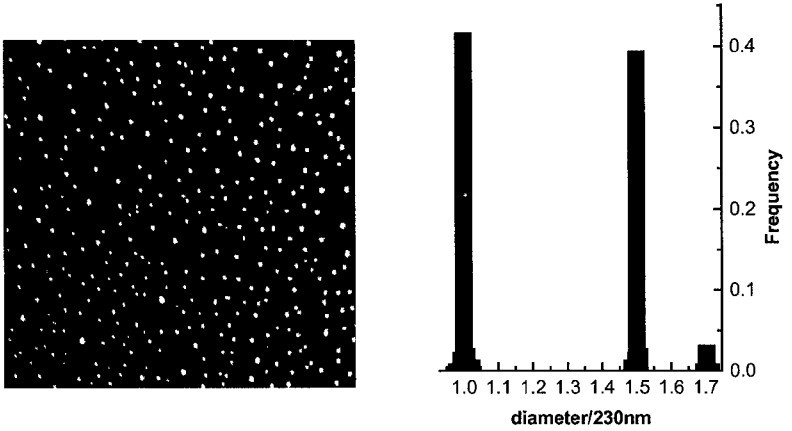


**Figure 3.** Scanning electron spectroscope of $CrO_2$ (major) and $Cr_2O_3$ (minor) nanoparticles deposited on soda-glass by laser-induced deposition in solution (LISD) (left) and the distribution diagram from the SEM image (right)

We did not know the exact nucleation and growth mechanisms in the laser-induced vapor and solution depositions yet. However, it is worthwhile to be further investigated. The preliminary AES and magnetic measurements of LISD deposited samples show similar results of these counterparts of OMCVD deposits – showing two phases rather than pure $CrO_2$ or $Cr_2O_3$. We will publish these results elsewhere due to the limitation to the length of this paper.

## CONCLUSIONS

We conclude in this presentation that we have used laser-initiated chemical vapor deposition and laser-induced solution deposition to successfully fabricate chromium oxide thin films and nanoparticles. The advantages of these techniques are selectively area deposition and strong texture growth as well as uniform deposits. Phase control of this system, at the surface or boundary layers, appears to be far more likely than the potential half metallic systems $La_{0.65}Sr_{0.35}MnO_3$ [21] and NiMnSb [22] where surface segregation readily occurs. The magnetization measurements show that the relative weight of both $Cr_2O_3$ and $CrO_2$ phases depends on and can be controlled by the oxygen partial pressure in the vapor deposition and by the selection of appropriate solute and solvents in the solution deposition.

## ACKNOWLEDGEMENTS

The authors would like to thank Dr. P.A. Dowben for his support and fruitful discussions during the progress of the project. Zhong's present research supported by the Louisiana Joint Faculty Appointment (JFAP) co-sponsored by Natural Science Foundation (NSF – EPSCoR program) and Louisiana Board of Reagents (LABOR). Cheng and Dowben's work was supported by NSF through grant # DMR-98-02126, the Center for Materials Research and Analysis (CMRA) and the Nebraska Research Initiative at the University of Nebraska.

## REFERENCES


1. A.M. Bratkovsky, Phys. Rev. **B56**, 2344 (1997).
2. S.S. Manoharan, D. Elefant, G. Reiss and J.B. Goodenough, Appl. Phys. Lett. 72, 984 (1998); X.W. Li, A. Gupta, T.R. McGuire, P.R. Duncombe, and Gang Xiao, J. Appl. Phys. **85**, 5585 (1999); K. Suzuki and P.M. Tedrow, Phys. Rev. **B58**, 11597 (1998).
3. J.D.M. Coey, A.E. Berkowitz, Ll Balcells, F.F. Putris and A. Barry, Phys. Rev. Lett. **80**, 3815 (1998).
4. J. S. Kouvel, D. S. Rodbell, J. Appl. Phys. **38**, 979 (1967).
5. K. Schwarz, J. Phys. **F 16**, L211 (1986).
6. S. Matar, G. Demazeau, J. Sticht, V. Eyert, and J. Kübler, J. de Physique **I 2**, 315 (1992).
7. M.A. Korotin, V.I. Anisimov, D.I. Khomskii and G.A. Sawatzky, Phys. Rev. Lett. **80**, 4305 (1998).
8. S. P. Lewis, P.B. Allen, and T. Sasaki, Phy. Rew. **B55**,10 253 (1997).
9. H. van Lueken and R.A. de Groot, Phys. Rev. **B51**, 7176 (1995).
10. E. Kulatov and I.I. Mazin, J. Phys. Condens. Matter. **2**, 343 (1990).
11. K.P. Kämper, W. Schmitt, G. Güntherodt, R.J. Gambino, and R. Ruf. Phys. Rev. Lett. **59**, 2788 (1987).
12. R. Weisendanger, H.-J. Güntherodt, G. Güntherodt, R.J. Gambino, and R. Ruf, Phys. Rev. Lett. **65**, 247 (1990).
13. R.J. Soulen, et al., Science **282**, 85 (1998); R.J. Soulen, et al., J. Appl. Phys. **85**, 4589 (1999).
14. W.J. DeSisto et al., Appl. Phys. Lett. **70**, 3789 (2000)
15. P. A. Dowben, et al., J. Appl. Phys. **67**, 5658 (1990).
16. K. Perkins, C. Hwang, M. Onellion, Yoon–Gi Kim, and P.A. Dowben, *Thin Solid Films* **198** (1991) 317–329
17. Derrick C. Mancini, et al., *J. Vac. Sci. Technol.* **B8**,1804 (1990).
18. D. Welipitiya, et al., Mat. Res. Soc. Symp. Proc. **475**, 257 (1997).
19. C. N. Borca, D. Welipitiya, S. Adenwalla, P. A. Dowben, Phys. Low-Dim. Struct. **11/12**, 173 (1997)
20. Z.C. Zhong, P.A. Dowben and D. J. Sellmyer, Materials Letters **37**, 320 (1998); Z.C. Zhong, V. Holmes, P.A. Dowben and D.J. Sellmyer, Mat. Res. Soc. Symp. Proc. (2000) pp 231; P.A. Dowben, Z.C. Zhong and D.J. Sellmyer, U.S. Patent No. 6,025,038, (15 February 2000).
21. H. Dulli, E. W. Plummer, P. A. Dowben, J. Choi and S-H, Liou, Appl. Phys. Lett. **77**, 88 (2000).
22. D. Riotoiu, J. P. Nozieres, C. N. Borca, B. Borca and P. A. Dowben, Appl. Phys. Lett. **76**, 2349 (2000).